

Abstract: The design of the shell and tube heat exchanger includes a tube-like shell with holes to which an inlet and outlet pipes are welded. Radial and tangential holes are produced manually by means of plasma cutting with the use of specialized tools, which determines high laboriousness of heat exchangers production. An automatic device is proposed to reduce the laboriousness of this operation. To produce the hole in the heat exchanger shell, two reversible motions are superimposed: linear motion of the cutter along the longitudinal axis of the shell and the shell rotary motion. A mathematical model of the required cutter motion is proposed, which describes the relative trajectories of the plasma cutter and the shell in parametric form. To verify theoretical premises, a prototype of the device was produced using a 3D prototyping technology, a ball screw for the reversible linear motion of the cutter and a stepper motor for the reversible rotary motion of the shell. The shell is fixed by means of a collet chuck and rests on the pipe roller support.

Keywords: passive safety, simulations, FEM

Streszczenie: Bezpieczeństwo bierne pojazdów jest jednym z ważniejszych problemów konstrukcyjnych. Rozwiązuje się go poprzez zastosowanie odpowiednich materiałów, głównie stali o bardzo wysokiej wytrzymałości i odpowiednie ukształtowanie elementów konstrukcyjnych. Niniejsze opracowanie przedstawia wyniki optymalizacji belki drzwi kabiny pojazdu N-Truck, projektowanego w ramach programu INNOMOTO, projekt nr: POIR.01.02.00-00-0194/16. Jako kryterium przyjęto graniczne wartości dopuszczalnych odkształceń elementów usztywniających oraz wartości naprężeń.

Słowa kluczowe: bezpieczeństwo bierne, symulacje, MES

Introduction

Steels with miscellaneous mechanical properties are the basic construction materials of the modern passenger cars body structure. The construction elements of the passenger car body are shown by the types and grades of their material on the Fig.1. The main construction material in the automotive industry is steel, despite the increasing use of aluminium alloys, magnesium, composite materials and plastics. This is mainly due to economic factors and the possibility of changing the properties of steel in a wide range. This helps to reduce vehicle weight and thus reduce fuel consumption while providing passengers with an adequate level of car passive safety. The hot and cold rolling stainless steels are common used in car body manufacturing. Annealing and normalizing after forming leads to ferritic steel structure. On the other hand the new steel generation needs the innovative forming process to get the more complex structure.

The traditional spot-welding technology is most popular until today, meanwhile laser welding and soldering, hybrid laser gluing, riveting technologies growing up [1].

Despite the expansion of technologies such as welding and laser soldering, hybrid laser, gluing, riveting and crimping resistive spot welding remains the main method of assembling the car bodies [1].

The steels used in the automotive industry can be divided into the following groups:

- I. mild, plastic, low carbon steels (DQSK, IF) with an ultimate strength of R_m below 300 MPa and elongation A of $30 \div 60\%$;
- II. Conventional steels with high strength HSS (BH, C Mn, IF with microadditives, HSLA) of $300 < R_m < 700$ MPa and reduced A compared to the previous group;
- III. Steels with very high strength AHSS (R_m above 700 MPa, up to 2000 MPa) and elongation range of $5 \div 30\%$, with the increase in strength goes with the reduction of plasticity;
- IV. High manganese steel TRIP/TWIP with very heavy strength up to 1200 MPa and very high plasticity.

The first two groups, known for many years, are materials used to build self-supporting car bodies on a mass scale manufacturing, due to good plastic properties. The steels of group III and IV are successively implemented into manufacturing and their share is steadily increasing, mainly in the passive safety elements.

The body structure consists of different profiles. By selecting their sections, shapes and materials, a controlled crushing zone accumulating the impact energy is obtained. A car body stiffness shall ensure the survivability of passengers. Guidelines for structural work

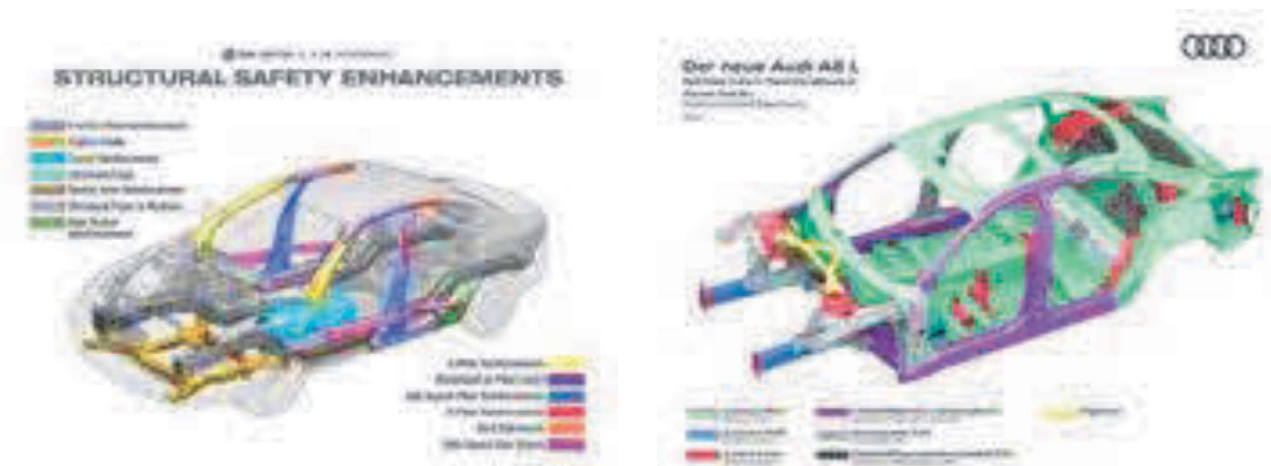


Fig. 1. The main structural materials of the cars bodies parts [3].
Rys. 1. Materiały konstrukcyjne użyte do produkcji istotnych elementów nadwozia pojazdu



Fig. 2. Left doors of the N-Truck car and reinforce elements
Rys.2. Drzwi lewej kabiny pojazdu N-Truck oraz element wzmacniający

are obtained of crash test results. Their methodology and evaluation criteria have been determined by the NCAP organization since 1996, which aims to harmonize the criteria used globally. It contains frontal, lateral and pedestrian impact tests. The results are announced to them after the completed attempts.

Verification test procedures

Spot tests and crash tests are the final verification of the solutions adopted. The General Motors' procedures have been adopted as guidelines for calculation methodology and criteria for assessing their performance in this work [6]. Vertical displacement f of the stamp at a constant speed of $v < 12.7 \text{ mm/s}$ ($0.5 \text{ } \ddot{7}\text{s}$) is inflicted on the final value $f_k = 152.4 \text{ mm}$ ($6 \text{ } \ddot{7}$). For displacements value $f_{\text{max}} = 115 \text{ mm}$, the beam reaction force F should be greater than $F(f_{\text{max}}) = 10 \text{ kN}$. The maximum beam strength (F_{max}) and the mean force (f_{av}), calculated as the ratio of the field under the $F(f)$ curve to f_k , shall also be determined. The simulation studies described below in the study are intended to shorten the time of finding the optimum shape and stiffness of the beam. In this work, the elastic modeling of the door frame was omitted due to lack of data.

Scope of the work

The work is carried out in the POIR. 01.02.00-00-0194/16 grant aiming to develop the design and manufacture of a prototype of an electric modular vehicle, with a DMC 3.5 t for transport in urban and industrial areas. This vehicle is temporarily named N-Truck.

Simulation works

Reinforce elements

The N-Truck door model was developed by MELEX and delivered as a step file to IMBiGS. The door view is shown in Fig. 2.

The possibility of mounting additional safety elements in the door space has not been provided, due to limited space. Therefore, the functions of the safety beam must be taken over the other parts, such as the window guide brackets and the door lock. These are shown in Fig. 2 by selecting green and brown.

Material properties

The each element of the beam were made of 2 mm thick Strenx 700 MC steel sheet. This is a hot rolled structural steel, with a minimum yield strength of $ReH = 700 \text{ MPa}$, dedicated for cold forming, enabling the more

Table 1. Strenx 700 MC Steel properties
Tabela 1. Właściwości mechaniczne stali Strenx 700 MC

Yield strength () min [MPa]	Ultimate strength Rm [MPa]	ElongationA80min % Probe thickness t < 3mm	Elongation A5min % Probe thickness t <3mm
700	750 - 950	10	12

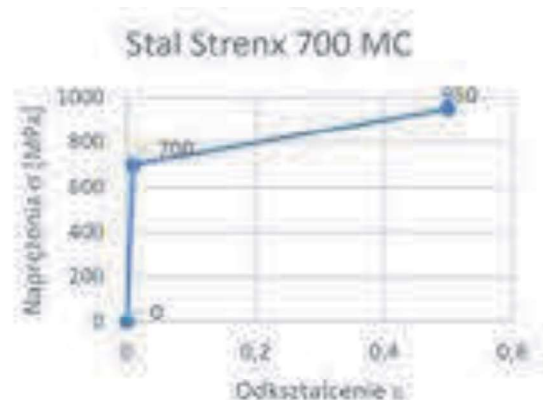
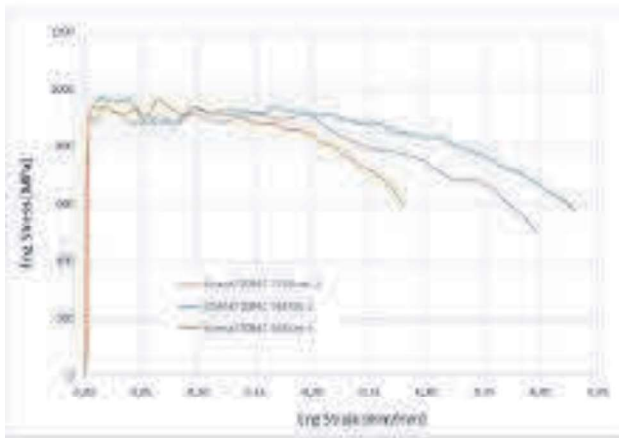


Fig. 3. Strenx 700 MC steel characteristic [5] and its model for simulation
Rys. 3. Charakterystyka stali Strenx 700 MC oraz model przyjęty do obliczeń.

powerful and lighter structures manufacturing. Strenx 700 MC meets and even exceeds the requirements for steel S700MC as in EN 10149-2 standard. The mechanical properties and the model of this steel adopted for the calculations are shown in tab. and in Fig. 3

MELEX beam simulation

Load

The door frame stiffness has not been taken into the model due to the lack of sufficient information. Due this, the fixed hinge and the fixed geometry were applied as the model constrains. The simulations were done for the conditions described in point "Simulation works". Such a model has been applied in the other cases concerned in this paper. The boundary conditions were worse than the real.

Results of simulation

Results of simulation were shown below.

The calculation results shown above show that the MELEX beam carries higher than recommended loads in the GM test. Unfortunately, its stiffness is too small, which is illustrated in two consecutive drawings. The stiffness criterion does not meet. Too little force was reached for 115 mm punch displacement. Its value is 1 740 N, which is more than 6 times less than required.

Conclusion

The door beam proposed by MELEX does not meet the requirements of these types of car components. First, it is not a technologically optimal design. It introduces additional operations to the manufacturing process, increasing its time and material intensity and thus the cost of manufacturing. Second, the results of the calculations carried out that the safety components made of STRONX 700 MC steel are capable of transferring higher than normative loads but do not meet the stiffness condition, which should eliminate them from the use. For this



Fig.4. MELEX beam. Stress distribution (Huber-Mises) and displacement
Rys. 4. Belka MELEX. Naprężenia zredukowane wg hipotezy Hubera-Misesa oraz przemieszczenia

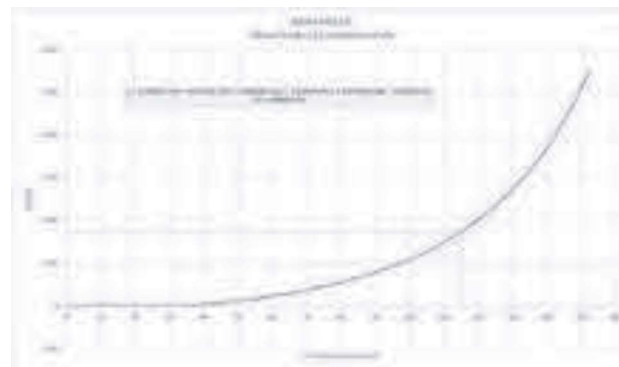
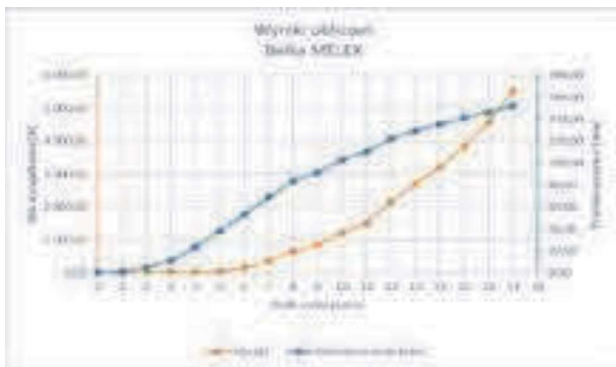


Fig. 5. MELEX beam. Displacement and reaction force in following calculation steps and force vs displacement
 Rys. 5. Belka MELEX. Przemieszczenia i wypadkowa siła reakcji w kolejnych krokach obliczeń oraz siła w funkcji przemieszczenia

reason, change their shape is necessary. The goal is to achieve more optimal stress distribution and improve the technology of the parts. In this second aspect it is about restrict the number of welding operations and replacing them with plastic machining or bending.

Beam optimizing, Beam No. 1,

Geometric model

The N.Truck door beam was based on a windshield lifting mechanism. As previously stated, additional space for reinforcing elements was not included. Therefore, they must fulfill a dual role: to protect the driver's space from lateral impact and to act as a support function for the mechanisms located inside the door (lock, windshield lifting mechanism, etc.). An additional assumption was the variability of the beam dimensions and the fixing points (Fig.6.). Therefore, the beam was made as a monolithic element of a steel sheet with 2 mm thickness. This parameter has a fixed value because it is the smallest thickness available at the supplier of the sheet.

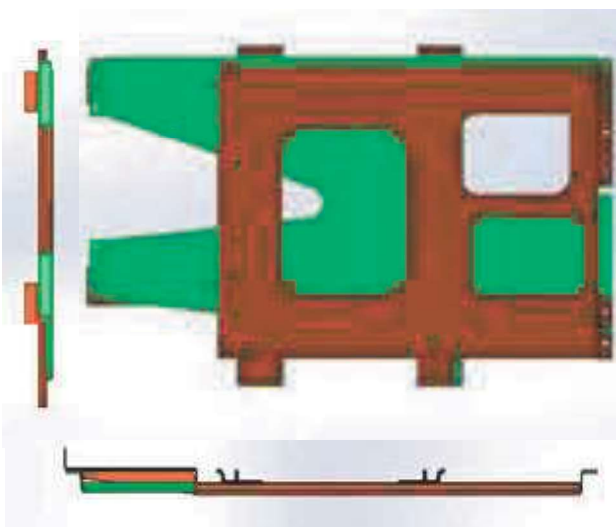


Fig. 6. The new shape of the beam, the primary in the background
 Rys. 6. Nowy kształt (kolor zielony) belki wzmacniającej na tle pierwotnej

The first concept of solution against the MELEX in the background is shown in Fig.6. The new reinforcement elements are marked with green color.

Simulation results

Results of simulation were shown below on Fig. 7.

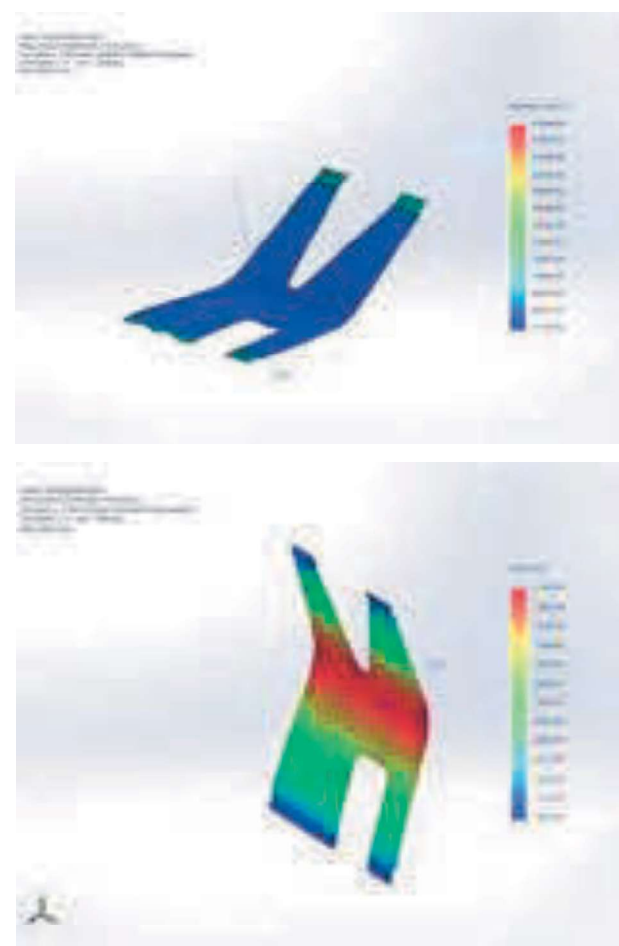


Fig. 7. Stress value. Stress distribution (Huber-Mises) and displacement
 Rys. 7. Naprężenia zredukowane wg hipotezy Hubera-Misesa oraz przemieszczenia

Force and displacement variation in time were show on Fig 8.

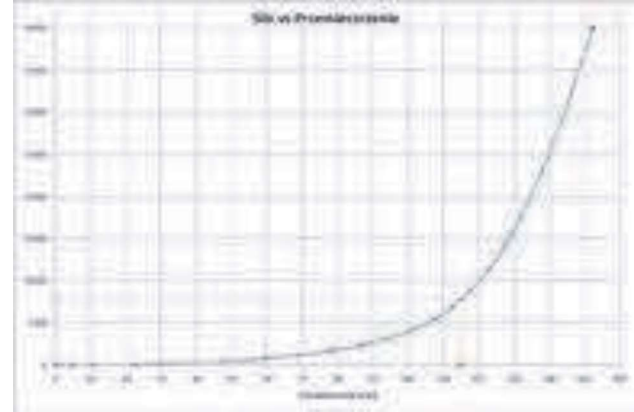
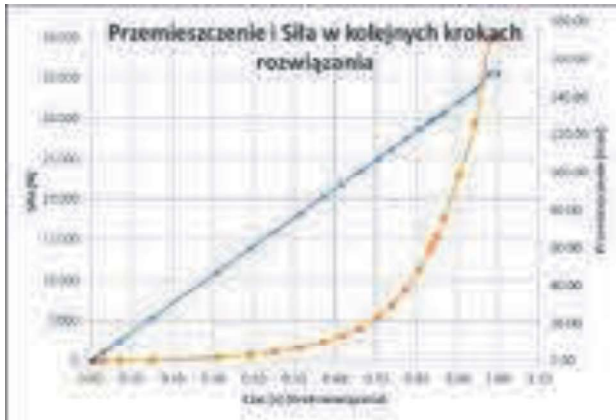


Fig.8. Displacement and reaction force in following calculation steps and force vs displacement
 Rys. 8. Zmienność siły i przemieszczenia w kolejnych krokach rozwiązania (czasu) oraz siła w funkcji przemieszczenia

Conclusions

The simulation results presented above show that the beam carries loads greater than those recommended in the GM test. Unfortunately, beam stiffness is too small, as illustrated in Fig. 8. The stiffness criterion is therefore not met. Force value at the 115 mm punch displacement is approx. 7 800 N, i.e. representing 78% of the minimum required value.

Beam optimizing. Beam No 2.

Geometric model

The optimization first step conclusions are used to new beam shape design. The goal is to make lower the beam cross section to obtain the plastic deformation at the smaller displacement values. A basic dimensions of the beam were shown on Fig. 9.

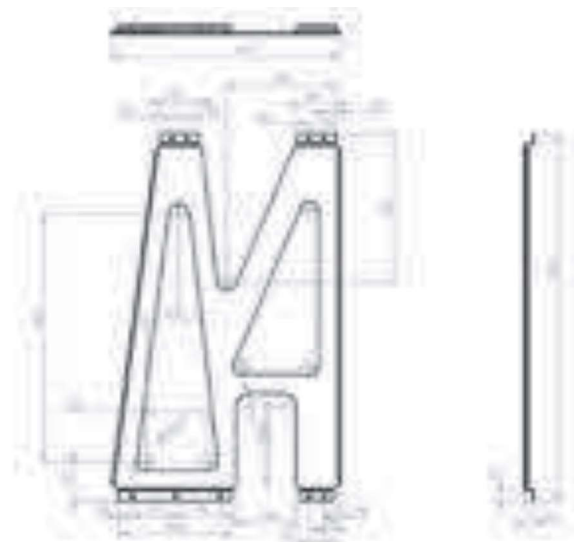


Fig. 9. Main beam dimensions – version 2
 Rys. 9. Podstawowe wymiary belki bocznej – wersja 2



Fig. 10. Beam 2. Stress distribution (Huber-Mises) and displacement
 Rys. 10. Belka 2. Naprężenia zredukowane wg hipotezy Hubera-Misesa oraz przemieszczenia

Results

Force and displacement variation in time were show on Fig 11.

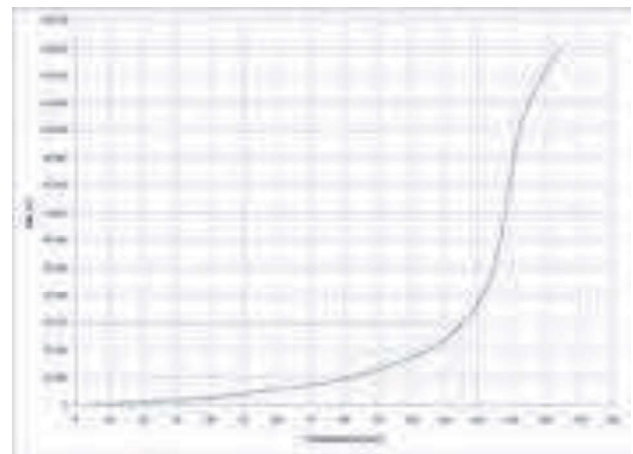
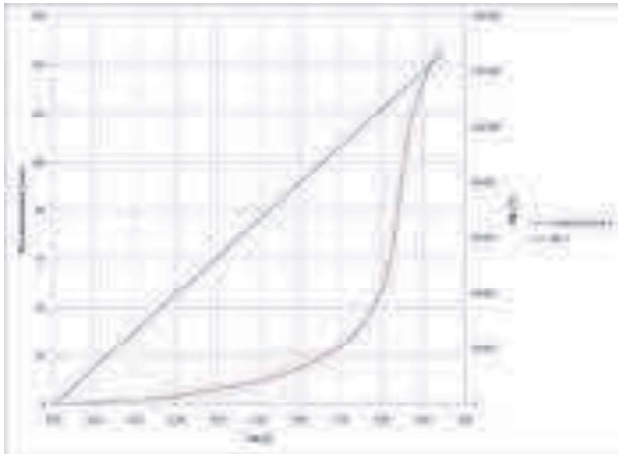


Fig. 11. MELEX beam. Displacement and reaction force in following calculation steps and force vs displacement
Rys. 11. Zmienność siły i przemieszczenia w kolejnych krokach rozwiązania (czasu)

Conclusions

The simulation results, as illustrate above, show that the "Beam 2" does not meet the strength requirements. Although for the punch displacement of 115 mm, the force value exceeds the minimum (almost threefold), however, the maximum strain is not achieved. The beam is destroyed before the 152.4 mm displacement value. The concentration of stresses with the highest values occurs at the beam fixing points. Hence it is necessary to redesign this beam area. It seems, the clamps are the critical part of beam.

Beam optimizing. Beam No 3.

Geometric model

Using the conclusions of the second optimization step, a new shape in the beam fixing area was designed. It was primarily driven by a change the damage mechanism of the element from the buckling to bending. Thus, the reinforcement of the upper surface (stiffening) was introduced by a 600 mm ball rolling of the with $R = 7,5$ mm radius in two beam areas and a 450 mm ball rolling with a radius of 10 mm, and a change of the tilt angle of the fastening feet from 90o up to 100o. A drawing with basic dimensions is shown below.

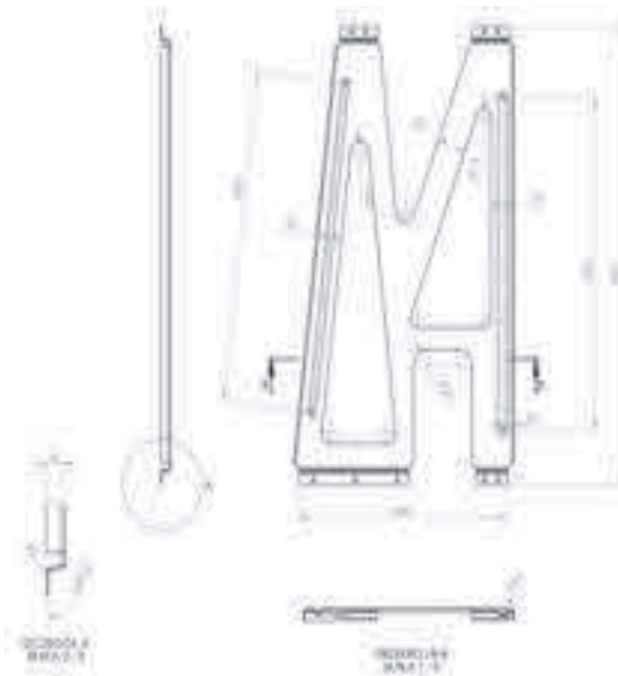


Fig. 12. Main dimension of the beam – version 3.
Rys. 12. Podstawowe wymiary belki bocznej – wersja 3



Fig. 13. Beam 3. Stress distribution (Huber-Mises) and displacement

Rys. 13. Belka 3. Naprężenia zredukowane wg hipotezy Hubera-Misesa oraz przemieszczenia

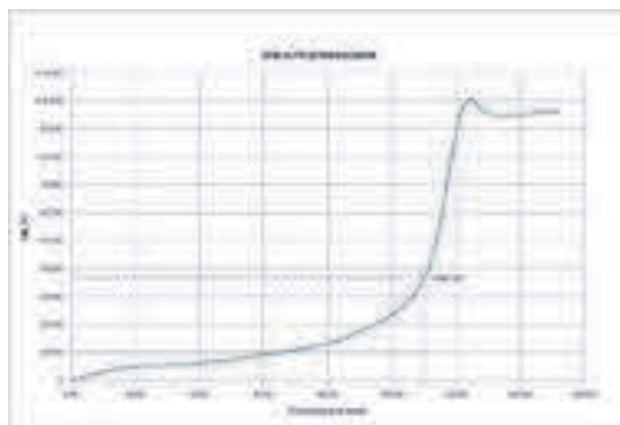
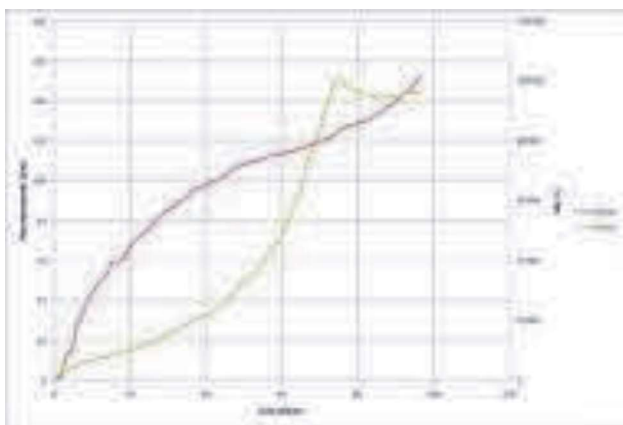


Fig. 14. Displacement and reaction force in following calculation steps and force vs displacement
 Rys. 14. Zmienność siły i przemieszczenia w kolejnych krokach rozwiązania (czasu) oraz zmienność siły w funkcji przemieszczenia

Simulation results

Stress and displacement distribution of the "beam 3" are shown on Fig.13.

Force and displacement variation in time are shown on Fig 14.

Conclusions

The calculation results shown that the "Beam 3" meets the strength requirements. As foreseen, the concentration of the stresses highest values occurs at the beam fixing holes. Tensile strength has been exceeded in the beam anchorage area. This can be caused by:

1. mesh errors, due to incorrect shape coefficient of elements generated near holes;
2. shell elements using instead of volumetric elements.

Thus, the final verification must take place on the stand tests.

References

[1] Senkra J., Współczesne stale karoseryjne dla przemysłumotoryzacyjnego i wytyczne technologiczne ich grzewania, PRZEGLĄD SPAWALNICTWA 11/2009

[2] <http://www.boronextrication.com/2009/01/14/2005-2009-buick-lacrosse-body-structure/>, dostęp 30.11.2018

[3] <https://automotive.arcelormittal.com/News/2791/AHSSforAudiA8>, dostęp 30.11.2018

[4] <https://www.e-autonaprawa.pl/artykuly/667/nadwozia-w-kolizjach-drogowych.html>, dostęp 30.11.2018

[5] HIPEBA: High Performance Steel for Safer and more-Competitive Barriers. RFSR-CT-2014-000212014

[6] STADNICKI J., WRÓBEL I., Poprawasztywności belki wzmacnienia tylnych drzwi samochodu osobowego, MECHANIK NR 7/2018

[7] <https://www.boronextrication.com/2012/01/10/2013-dodge-dart-body-structure/> dostęp 30.11.2018

This paper was realized in the POIR.01.02.00-00-0194/16 grant "N.Truck a modular electric utility vehicle with GVW up to 3,5 t used for transport in urban and industrial area"

mgr inż. Andrzej Barszcz – Instytut Mechanizacji Budownictwa i Górnictwa Skalnego, 04-697 Warszawa, ul. Mrówcza 243, e-mail: a.barszcz@imbigs.pl

dr inż. Mirosław Chłosta – Instytut Mechanizacji Budownictwa i Górnictwa Skalnego, 04-697 Warszawa, ul. Mrówcza 243, e-mail: m.chlosta@imbigs.pl

PORTAL INFORMACJI TECHNICZNEJ
największa baza publikacji on-line
www.sigma-not.pl